Critical particle size for fractionation by deterministic lateral displacement

David W. Inglis,*[a] John A. Davis,[a] Robert H. Austin[b] and James C. Sturm[a]

Received 1st November 2005, Accepted 2nd March 2006
First published as an Advance Article on the web 17th March 2006
DOI: 10.1039/b515371a

The fractionation of small particles in a liquid based on their size in a micropost array by deterministic lateral displacement was recently demonstrated with unprecedented resolution (L. R. Huang, E. C. Cox, R. H. Austin and J. C. Sturm, *Science*, 2004, **304**, 987–990, ref. 1). In this paper, we present a model of how the critical particle size for fractionation depends on the micropost geometry, depending specifically on the gap between posts, the offset of posts in one row with respect to another, and whether the fluid is driven by hydrodynamics or by electroosmosis. In general the critical particle diameter is much smaller than the gap, which prevents clogging. The model is supported by data with particles from 2.3 to 22 μm.

Introduction

Microfabricated post arrays have recently been used to continuously separate a stream of different sized particles in fluid using a principle known as "deterministic lateral displacement".[1] Previous work has shown that this technique can separate particles of 0.8 to 1 micron diameter with resolution greater than one percent. This ability and the simplicity of the device will likely lead to a wide range of applications for both biological and non-biological separations.[2,3] The goal of this paper is to provide a theory and experimental measurements of the separation conditions where the flow is driven by pressure differential, *i.e.* hydrodynamically.

Deterministic lateral displacement does not rely on diffusion, but instead, particles above and below a critical size follow different, reversible, predetermined paths through an array of posts. It is possible to continuously separate a range of particle sizes by placing arrays of different critical particle sizes in series.

The row shift fraction, ε, is defined as the ratio of the horizontal distance that each subsequent row is shifted, $\varepsilon\lambda$, divided by the array period, λ (Fig. 1). In this paper the vertical row spacing is also λ so the columns of posts are at a slope ε to the average direction of flow.

Theoretical analysis

As described by Huang *et al.*,[1] the total fluid flux through each gap can be divided into $n = 1/\varepsilon$ flow streams, where n is a whole number. Each flow stream carries equal fluid flux, shown schematically in Fig. 1 for $n = 3$. The streamlines are separated by stall lines, each stall line beginning and ending on a post. The streamlines shift their positions cyclically so that after n rows each streamline returns to its initial position within the gap. In Fig. 1, streamline 1 moves to position 3 in the next row, position 2 in the row after that, and finally back to position 1 after three rows. The first and second streamlines are always bifurcated by a post in the subsequent row.

If a particle's radius is larger than the width of the first streamline, the particle will be forced to remain in the second or higher numbered streamline in every row. It will be bumped

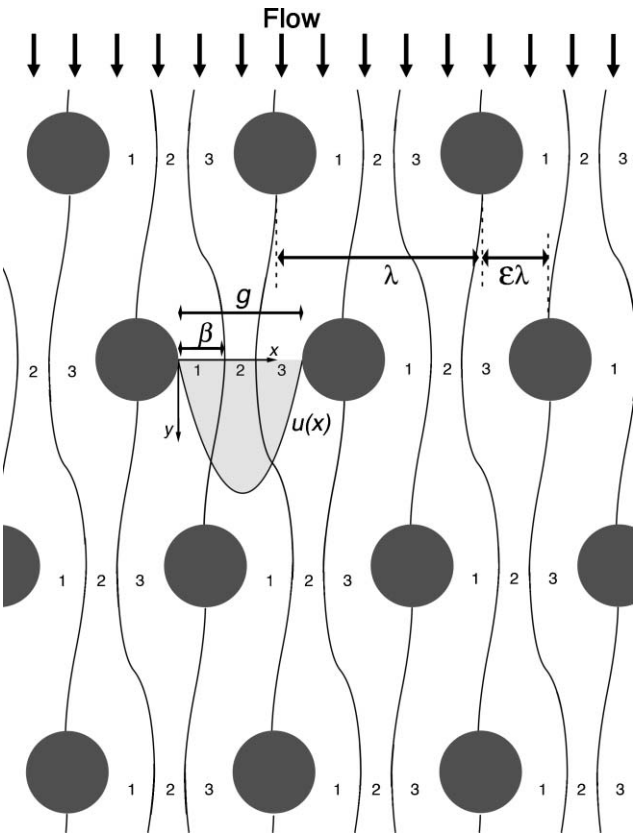

Fig. 1 Top view diagram of streamlines in low Reynolds number flow through an array of infinitely tall posts. Each row is shifted to the right by one third of the post-to-post spacing, λ, making the row shift fraction $\varepsilon = 0.33$. Three equivalent streamlines flow between each gap, numbered 1 to 3, which cyclically permute from row to row. The streamlines are divided by stall lines which begin and terminate at the posts. An example flow profile $u(x)$ is drawn into one of the gap regions. β is the width of the first streamline.

[a]*Princeton Institute for the Science and Technology of Materials, PRISM Princeton University, Princeton, NJ, 08544, USA. E-mail: dinglis@princeton.edu*
[b]*Princeton University Department of Physics, Princeton, NJ 08544, USA*

deterministically by $\varepsilon\lambda$ at each subsequent row, thus traveling in "bump mode." If a particle's radius is less than the width of the first streamline, it will follow the cyclic procession of the streamlines and travel in "zigzag" mode. The critical particle radius is the dividing line between the two modes of travel and in this model is equal to the width of the first streamline, which we define as β. The parameter of interest is the critical particle diameter, D_c, which is twice the radius or twice the width of the first streamline, β.

The critical particle diameter, D_c, for determining which path a particle will follow is then phenomenologically given by

$$D_c = 2\beta \tag{1}$$

We can replace β to show the effect of the gap, g, and the row shift fraction, ε:

$$D_c = 2\eta g\varepsilon, \tag{2}$$

but then we must include the variable parameter η to accommodate for non-uniform flow through the gap.

To calculate the width of the first streamline, and the critical particle radius, for any array we integrate the flow profile, $u(x)$, starting from zero at the post edge to β (Fig. 1). Each streamline carries equal fluid flux, but is not necessarily the same width. If β is defined to be the width of the first streamline, then this integral must equal ε times the total fluid flux.

$$\int_0^{\beta} u(x)\,\mathrm{d}x = \varepsilon\int_0^{g} u(x)\,\mathrm{d}x \tag{3}$$

The shape of the flow profile determines the widths of the streamlines and thus β. By assuming a conventional parabolic flow profile through the gap, with zero velocity at the post sidewalls, it is possible to analytically find the width of the first stream line, β, as a function of ε. Such flow occurs for hydrodynamic flow through a narrow slit.[4] The flow profile $u(x)$ can be written

$$u(x) = \left[\frac{g^2}{4} - \left(x - \frac{g}{2}\right)^2\right]. \tag{4}$$

Solving eqn (3) involves finding the cube root of:

$$\left[\frac{\beta}{g}\right]^3 - \frac{3}{2}\left[\frac{\beta}{g}\right]^2 + \varepsilon\frac{1}{2} = 0. \tag{5}$$

Using $D_c = 2\beta$, one can write the solution to the cubic equation as:

$$D_c = g\left[1 + 2w + \frac{1}{2w}\right], \tag{6}$$

where

$$w^3 = \frac{1}{8} - \frac{\varepsilon}{4} \pm \sqrt{\frac{\varepsilon}{16}(\varepsilon - 1)} \tag{7}$$

and the correct root of w^3 is

$$w = \left[\frac{1}{8} - \frac{\varepsilon}{4} + \sqrt{\frac{\varepsilon}{16}(\varepsilon - 1)}\right]^{(1/3)}\left(-\frac{1}{2} - \mathrm{i}\frac{\sqrt{3}}{2}\right). \tag{8}$$

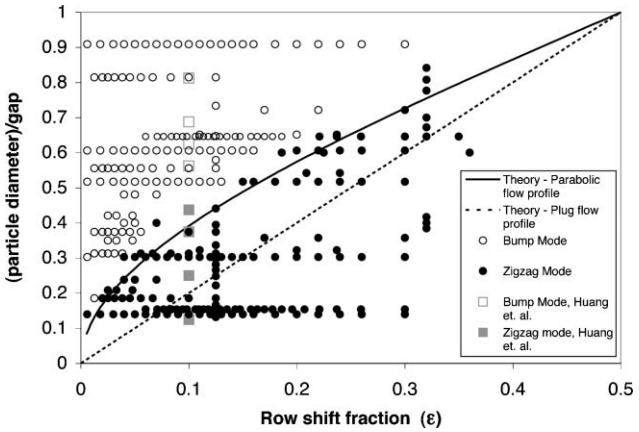

Fig. 2 Experimental points of the particle diameter divided by the gap, versus the row shift fraction, ε. For this work (in black) and that of Huang *et al.*[1] (in grey), open points represent bump mode and solid points represent zigzag mode. Zigzag mode particles follow the streamlines, while bump mode particles follow the array slope, ε.

An analytical expression for η is then

$$\eta = \frac{D_c}{2g\varepsilon}. \tag{9}$$

The fraction $\frac{D_c}{g}$ from eqn (6) is plotted as a solid line in Fig. 2. For $\varepsilon = 0.1$ the predicted critical particle diameter is $0.4g$, $\eta = 2.0$. For $\varepsilon = 0.01$ the predicted critical particle diameter is $0.12g$ and $\eta = 5.9$. The surprisingly large critical size at small ε is because at small ε the first streamline contains only very slowly moving fluid in relation to the streamlines in the middle of the gap, so the first streamline must be wider than the others to carry the same fluid flux as streamlines with higher velocities. The parameter η (eqn (9)) obtained by assuming a parabolic flow profile (eqn (4)) is plotted as a solid line in Fig. 3. The parameter η increases with decreasing row shift fraction, and goes to unity for the largest meaningful row shift fraction, $\varepsilon = 0.5$.

In the unique case where the flow profile is uniform across the gap (plug flow), each streamline would be $g\varepsilon$ wide. Then

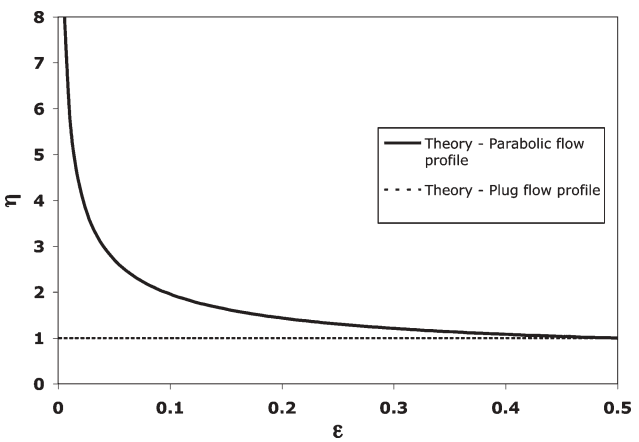

Fig. 3 Plot of the variable parameter $\eta = \frac{D_c}{2\varepsilon g}$ which describes the ratio of critical particle diameter to row shift fraction, ε, times gap size, g, for both parabolic and plug flow profiles.

the critical particle diameter would be $2\varepsilon g$, and the η parameter would be unity, shown in Fig. 3 as a dashed line. Fluid driven electroosmotically is expected to have a profile more closely resembling plug flow than fluid driven by a hydrodynamic pressure gradient.

Experiment

Devices with a variety of shift fractions and gap sizes were fabricated so that the effect of changing the shift fraction, ε, and the gap, g, on the critical particle size could be observed. The devices consisted of a central region of posts, bounded above by many narrow channels that inject fluid, and below by similar channels to carry fluid away, as in Fig. 4. Holes were sand-blasted through the silicon substrate to allow for back-side fluid connections.

The lithographically defined values of ε ranged from 0.01 to 0.33. The distance between posts, g, ranged from 12 to 38 μm. The post size to gap size ratio ranged from 0.32 to 1.36. The data were collected from bead separations performed on three separate devices, each with up to 22 combinations of g and ε in series. The features of the devices were etched into silicon substrates to a depth of at least 25 μm, with a sidewall angle of less than 2°. Vertical average flow through the array is set by applying a uniform fluid flux across the top and bottom by high fluidic resistance channels upstream and downstream of the array, Fig. 4.[5]

The devices were sealed with polydimethyl siloxane (PDMS) (GE Silicones, Wilton, CT) coated glass cover slips. The devices were soaked in a 2 g L^{-1} solution of Pluronic F108 (BASF, Mount Olive, NJ). Polystyrene beads (Duke Scientific, Palo Alto, CA, and Bangs Laboratories, Fishers, IN) with diameters ranging from 2.3 to 22 μm were injected into the arrays through a central reservoir and analyte injection channel. A hydrodynamic jet was formed in the array and the beads were observed to travel in either the bump or the zigzag mode. The average bead velocity was between 500 and 1500 μm s^{-1}, achieved by pressure differentials from one end of the chip to the other of approximately 3 to 14 kPa (0.5 to 2 psi). Observations were made using a Nikon inverted epifluorescence microscope (Thunder Bay, CA).

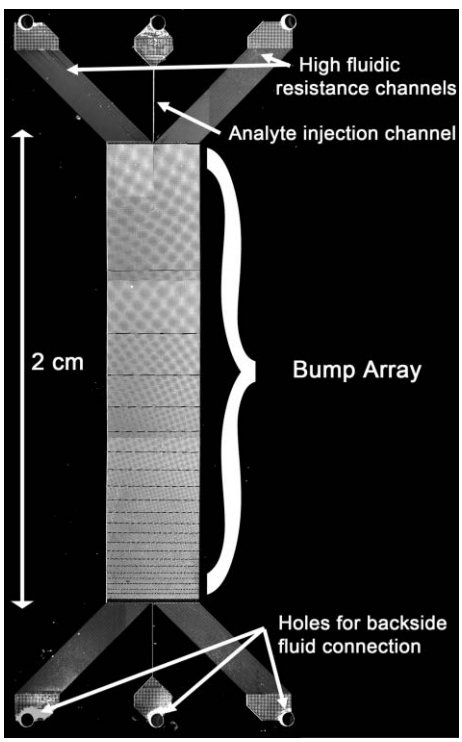

Fig. 4 Top view image of etched silicon device showing central bump array, high fluidic resistance channels, analyte (bead solution) injection channel, and sand-blasted holes for backside fluid connections.

Fig. 2 shows a collection of points, each one corresponding to one combination of particle size, gap and shift fraction. The particle diameter divided by the gap is plotted on the vertical axis, and the shift fraction, ε, is plotted on the horizontal axis. If the particle moved in the zigzag mode it was plotted as a filled circle. Particles moving in the bump mode were plotted as open circles. Points from ref. 1 were also plotted. The distribution in size of the bead populations was apparent on a number of occasions. At 8 of the 297 different combinations of gap, ε and nominal bead diameter, the beads showed mixed behavior, some beads traveling in zigzag mode and others in bump mode. These data points are not included in Fig. 2 for clarity.

There is a clear division between particles which zigzag or bump, with larger particles bumping. As ε increases the critical size increases as the width of the first streamline increases.

Discussion

In Fig. 2 the general agreement between the theoretical critical diameter (eqn (6)) and the experimentally observed dividing line between zigzaging and bumping particles is good. As ε increases the critical particle diameter increases. The critical particle size is larger than that implied by plug flow ($\eta = 1$) and in better agreement with that predicted by a parabolic flow profile, as expected for a fluid profile where the fluid velocity is zero at any surface, *i.e.* a no-slip condition. For fluid flow where the velocity at the post surface is not zero, as in electroosmotic flow, the critical particle diameter is expected to be lower, closer to the plug flow theory. As expected, the results to first order do not depend on flow speed or gap size. Note both models (and the data trend) converge at a critical diameter equal to the gap as ε reaches 0.5. In this mostly impractical case there are only two streamlines, each with equal fluid flux.

One now has a clear design guide for designing these separation devices. An important question in bump array design is how to separate a wide range of particles without clogging. The largest particle that can be separated must be less than the gap, g, and the smallest particle that can be separated is given by the critical diameter, D_c, of the section with the smallest ε. Practical limitations arise at the small sizes since very low ε sections must be extremely long to achieve significant lateral separation, and at the large sizes from bead clogging. Bead clogging is significant for beads nearly as big as the gap size and is made worse by higher bead densities. Further difficulties arise for sub-micron sized particles as the effects of Brownian motion and diffusion increase. A smaller particle will diffuse out of its streamline more rapidly, necessitating a larger separation angle and a higher fluid

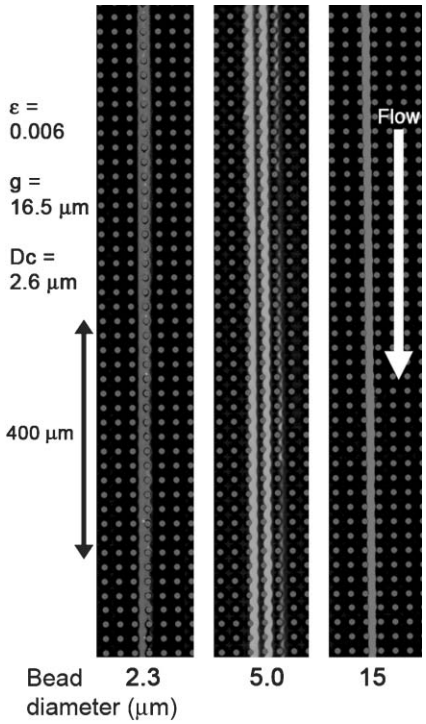

Fig. 5 False color images showing zigzag and bump mode flow of fluorescent polystyrene beads in an array with $\varepsilon = 0.006$, a gap of 16.5 μm (25 μm pitch), and a critical diameter, D_c, of 2.6 μm. The 2.3 μm beads are below the critical particle size and thus travel vertically in zigzag mode. The 5.0 and 15 μm beads are above the critical particle size and so travel in bump mode at a slight slope of 0.006 to the vertical flow. Although the 15 μm particles are nearly six times the critical diameter they do not, in general, clog the array and flow through it in zigzag mode.

velocity, yet achieving higher velocities at smaller gaps is difficult as the velocity through a slit scales as one over the gap squared.

In Fig. 5 we show 5.0 μm particles traveling in the bump mode of an array with a 16.5 μm gap, and $\varepsilon = 0.06$. The 2.3 μm particles are below the critical diameter, $D_c = 2.6$ μm. This demonstrates how an array with a very low ε can have a critical particle diameter, D_c, much smaller than the gap. Placing this array in series with arrays of larger ε makes the continuous separation of particles over a wide size range possible. We expect, when diffusion is negligible, that particles with diameters as small as one fifth of the gap should be separable with resolution approaching 1%. This improvement in the dynamic separation range may be useful in many areas including the separation of in-homogeneous biological samples. Increasing the separation range of a device comes at some cost. The length of the device must be increased and size resolution may be lost.

Conclusion

Theoretical models for the critical particle size of fractionation in deterministic lateral displacement separation arrays have been presented, with the main parameters being the row shift fraction, ε, and the ratio of particle to gap size. Devices with a parabolic flow profile through the gap due to pressure driven flow have a larger critical diameter than that expected for fluid driven by electroosmotic flow. A wide range of experiments under pressure-driven conditions support the parabolic flow model. These experiments indicate a maximum possible separation range of around 5 in a single array. Separations with a larger range can be accomplished by using multiple devices.

Acknowledgements

This work was supported by grants from DARPA (MDA972-00-1-0031), NIH (HG01506), (E21F46G1), NSF Nanobiology Technology Center (BSCECS9876771) and the State of New Jersey (NJCST 99-100-082-2042-007). We acknowledge support from the Cornell University National Fabrication Center, where the some of the deep silicon etching was performed. We also thank Prof. S. Chou and Keith Morton for use of their deep silicon etcher.

References

1 L. R. Huang, E. C. Cox, R. H. Austin and J. C. Sturm, *Science*, 2004, **304**, 987–990.
2 S. Zheng, R. Yung, Y. Tai and H. Kasdan, *Proceedings of IEEE MEMS*, Miami Beach, FL, USA, 2005, pp. 851–854.
3 S. Zheng, Y. Tai and H. Kasdan, *Proceedings of μTAS*, Boston, MA, USA, 2005, pp. 385–387.
4 J. P. Brody, P. Yager, R. E. Goldstein and R. H. Austin, *Biophys. J.*, 1996, **71**, 3430–3441.
5 N. Darnton, O. Bakajin, R. Huang, B. North, J. O. Tagenfeldt, E. C. Cox, J. Sturm and R. H. Austin, *J. Phys.: Condens. Matter*, 2001, **13**, 4891–4902.

